Astron. Astrophys. 351, 1003–1015 (1999)

ASTRONOMY AND ASTROPHYSICS

The stellar content of soft X-ray surveys

II. Cross-correlation of the ROSAT All-Sky Survey with the Tycho and Hipparcos catalogs

P. Guillout[1,2], **J.H.M.M Schmitt**[3], **D. Egret**[1], **W. Voges**[2], **C. Motch**[1], **and M.F. Sterzik**[4]

[1] Observatoire Astronomique, CNRS UMR 7550, 11 rue de l'Université, 67000 Strasbourg, France
[2] Max-Planck-Institut für Extraterrestrische Physik, 85748 Garching, Germany
[3] Universität Hamburg, Hamburger Sternwarte, Gojenbergsweg 112, 210029 Hamburg, Germany
[4] European Southern Observatory, Casilla 19001, Santiago 19, Chile

Received 18 May 1999 / Accepted 22 September 1999

Abstract. We present the result of the cross-correlation of the ROSAT All-Sky Survey with the Tycho and Hipparcos catalogs. The constructed *RASS - Tycho* (RasTyc) and *RASS - Hipparcos* (RasHip) samples respectively consist of 13 875 and 6 200 matches and represent the largest and most comprehensive samples of stellar X-ray sources constructed so far. The X-ray horizon allows to probe distances up to about 200 pc for F - G RasTyc - RasHip stars younger than 100 Myr but only to 80 pc or less for older ones. The magnitude limit of the optical catalogs determine the horizon for K - M RasTyc - RasHip stars which are sampled only within about 50 pc (or less) of the Sun whatever their ages are. We compare the Hipparcos and RasHip HR-diagrams and discuss the differences. X-ray selection strengthens the Zero Age Main Sequence but evolved stars are detected as well. We compute detection rate, mean Fx/Fopt and X-ray luminosity with an unprecedented color bin resolution for *on* (between the Zero and Terminal Age Main Sequence i.e. class V) and *off* (above the Terminal Age Main Sequence i.e. class III) main sequence regions. Once corrected for Fx/Fopt bias, the detection rate is remarkably constant for G-M *on* main sequence stars but reveals a peak of detection for F-type stars. Detection rate in the A-type stars region is compatible with those computed for F-M stars, as expected if a late type companion is responsible for the X-ray emission. High mass stars evolving along the post-main sequence evolutionary tracks are clearly detected in the main sequence turnoff and blue part of the "clump" while no significant detection arises on the cool side. Theoretical considerations naturally explain these observations. We address the question of the presence of very young stars in the solar neighborhood and derive an upper limit on the number of "possible" *isolated* pre-main sequence stars in the RasTyc-RasHip samples. Finally we discuss briefly the pending questions for which the RasTyc and RasHip samples are likely to give new insight.

Key words: stars: late-type – Galaxy: stellar content – X-rays: stars

Send offprint requests to: P. Guillout (guillout@astro.u-strasbg.fr)

1. Introduction

The discovery that stars of almost all spectral types were X-ray emitters with luminosities in the range 10^{26} - 10^{34} erg s^{-1} was one of the major unexpected results of the Einstein mission (Vaiana et al. 1981). The ROSAT satellite launched in 1990 has undoubtedly confirmed and completed the picture drawn with the Einstein Observatory. The knowledge of the composition of the high and low galactic latitude soft X-ray sky is partly based on the investigations of the Einstein Medium Sensitivity Survey (EMSS, Gioia et al. 1990, Stocke et al. 1991) and to a larger extent based on the ROSAT All-Sky Survey (RASS, Voges 1992). The general path to explore this unprecedented amount of data consists in systematic optical identification of X-ray sources in small size regions (typically smaller than a few hundred deg^2) in order to estimate at least statistically the X-ray content of the sky as seen by ROSAT. Detailed investigations of low and high galactic latitude test regions show that young active late type stars (F-M) represent respectively from 85% (Motch et al. 1997) to 30% (Zickgraf et al. 1997) of the RASS soft X-ray sources. The RASS thus appears as a piece of choice to study the properties of young stars in the solar neighborhood and especially their large scale (meaning all-sky) distribution. However a major problem encountered in multi-wavelength analysis of large samples is that the optical identification generally required for all candidates is a very long and time consuming task. Especially if one needs many parameters (magnitude, color, parallax...) then the task is far beyond our present ground capabilities.

An alternative and easier approach is the cross-correlation of the RASS sources positions with astronomical catalogs which allow to construct samples of objects with known X-ray and optical properties. The choice of the input catalog is fundamental to determine the class of object (star, galaxy, cataclysmic variable...) and also because any bias present in it is propagated into the constructed sample.

This paper is dedicated to the first step of a research project lying at the crossroad of the RASS and Tycho/Hipparcos catalogs, based on two major spatial experiments of the last ten years flown on the ROSAT and Hipparcos satellites respectively.

While ROSAT gathered X-ray photons from X-ray sources over the whole sky, the Tycho mission took advantage of the star mappers on board Hipparcos in order to measure magnitude and position of the brightest one million stars over the whole celestial sphere. The cross-correlation of the RASS with the Tycho/Hipparcos catalogs provided us with the largest samples of stellar X-ray sources statistically identified so far (RasTyc and RasHip samples respectively). This drastically improves the quality of the optical parameters and also supplies homogeneous parallaxes and accurate proper motions for X-ray sources successfully cross-correlated with stars. In this paper we describe in details the construction and characteristics of the two samples as well as their bias. We compute and discuss detection rate throughout the HR diagram and show that these observations can be considered as an observational test of the dynamo theory. We also address the question of *isolated* T-Tauri stars in the solar neighborhood. With its very accurate optical data the RasHip sample offers the possibility to study in details the dependence of stellar X-ray emission with internal structure and physical conditions (Guillout et al. 1999 in preparation, paper III). On the other hand, with its unprecedented sky coverage the RasTyc sample allows to probe the nearby galactic structure and evolution within the last Gyrs (Guillout et al. 2000 in preparation, paper IV) by comparison with stellar X-ray population model (Guillout et al. 1996a, paper I).

This paper is organized as follows: in Sect. 2 we briefly recall the main characteristics of the RASS and Tycho/Hipparcos catalogs; Sect. 3 presents the RasTyc and RasHip samples and their X-ray and optical bias; Sect. 4 deals with the X-ray selected HR diagram and detection rate; the question of the isolated pre-main sequence population is discussed in Sect. 5; Sect. 6 briefly presents the pending questions for which the RasTyc and/or RasHip samples are likely to give new insight; conclusions and perspectives are drawn in Sect. 7.

2. The RASS and Tycho/Hipparcos catalogs

2.1. The RASS source list

The ROSAT All-Sky Survey (Voges 1992) was carried out during the first six months of the ROSAT mission from 1990 July till 1991 February. At this occasion, the Position Sensitive Proportional Counter (PSPC) was moved in the focal plane of the X-ray Telescope (XRT). A review of the main characteristic of the ROSAT satellite and instrumentation can be found in Trümper (1983) and Pfeffermann et al. (1986). The ROSAT PSPC has 255 instrumental energy channels sensitive from 0.1 to 2.4 *keV* (broad band). The spectral resolution of the XRT + PSPC configuration permits a reasonable spectral analysis in three energy bands although better spectral resolution is possible for bright X-ray sources or deep exposure. The source detection using the maximum likelihood (ML) technique (see Voges et al. 1999) was done in these three bands allowing to compute for each source the HR1 and HR2 hardness ratio. About 150 000 sources were detected during the survey at a maximum likelihood ML ≥ 7. As shown in Fig. 6 of Voges (1992) from preliminary analysis of the RASS, the density of the X-ray sources is nearly constant over the whole sky suggesting some 'conspiracy' of the stellar and extragalactic populations which apparently roughly balance their contribution with varying galactic latitude.

2.2. The Hipparcos and Tycho catalogs

The Hipparcos and Tycho catalogs (ESA 1997) are based on observations performed during the whole Hipparcos spacecraft mission from November 1989 to March 1993. Exceeding their basic role of estimating the attitude for the main mission, the satellite star mappers were used to produce an additional catalog known as the Tycho experiment. Resulting of the complete scanning of the celestial sphere over three years, the Tycho program performed an all-sky survey of all stars down to about eleven magnitude (i.e. one million stars) while the Hipparcos main mission focused on the about 118 200 objects of the *Hipparcos Input catalog* (ESA 1993). Differences in the content, astrometric and photometric accuracies reflect the specific acquisitions and reductions techniques of each experience. Despite the unexpected problem arising with the apogee engine the mission was a success, all of the scientific goals adopted in 1980 being surpassed. The following subsections briefly present the Hipparcos/Tycho data types relevant for our study, the reader being encouraged to consult the Hipparcos and Tycho documentation (ESA 1997, vol.4; Høg et al. 1997) for additional information.

2.2.1. Astrometric data

Although of lower astrometric quality than the Hipparcos data (< 1 mas), the Tycho catalogue also provides astrometry (position and proper motion in a quasi-inertial reference frame and absolute parallaxes) for slightly more than one million stars. The median astrometric precision ≈ 25 mas is at least as accurate as that reached by ground based meridian instruments but concerns an homogeneous sample with an unprecedented mean sky density of ≈ 25 per square degree. The astrometric errors strongly depend on star magnitude but do not exceed 5 mas for the brightest objects.

2.2.2. Photometric data

In addition to astrometry the Tycho experiment acquired two color photometric data referred to as Tycho magnitudes, B_T and V_T closely corresponding to the Johnson B and V magnitudes respectively. The limiting magnitude is $V_T \approx 11.5$ and the Tycho catalogue is mostly complete up to a limit of about $V_T = 10.5$ ($\geq 90\%$ at this limit, Egret & Fabricius 1997). The median standard error is less than 0.01 mag for stars brighter than $V_T = 8$ but exceeds 0.08 mag for the fainter ones. The Tycho catalog is thus presently the largest photometric survey in two colors ever made. On the other hand Hipparcos only measured the so-called H_p magnitude (passband 3 400 - 8 900 Å, see ESA 1997, vol.1 Table 1.3.5 and Table 1.3.6 for relation with V magnitude) but with an unprecedented accuracy (0.0015 mag for $H_p < 9$).

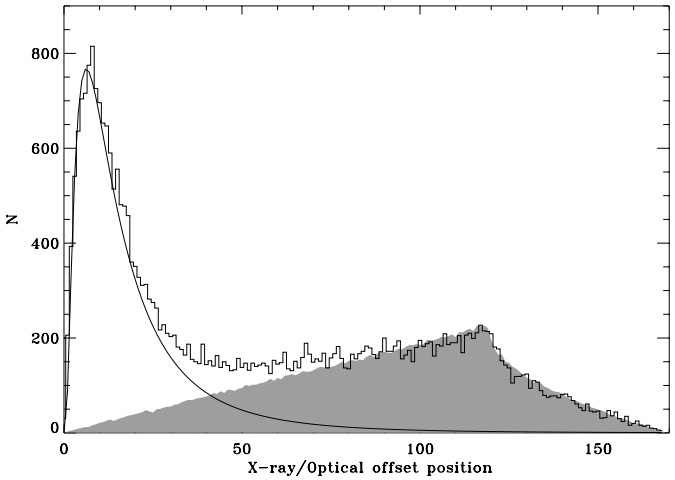

Fig. 1. Distribution of X-ray/Optical offset position (arcsec) for the 32 234 closest matches resulting from the cross-correlation process of the RASS and Tycho catalogs. The full line is the best fit of a log normal to the distribution of the expected physical matches. It is noticeable that the simulation of the expected spurious population (grey shaded area) perfectly reproduces the decrease of the matches beyond 2 arcmin which is due the box shaped surface adopted for the correlation of the catalogs. We define the *RASS - Tycho* sample as the 13 875 matches with associated position offset less than 30 arcsec.

Table 1. Number of RASS - Tycho matches as a function of the X-ray/Optical offset position Dxo (arcsec). The expected fraction of spurious matches f_{spu} as well as the fraction of physical matches f_{phy} = 1 - f_{spu} are also quoted.

Dxo	N	f_{phy}	f_{spu}
20	11290	92.82	7.18
30	13875	92.74	7.26
40	15498	90.04	9.96
50	16854	86.62	13.38

2.2.3. Other relevant data

Due to the scanning method, about 100 individual photometric observations in the H_p, V_T and B_T channels were acquired for each star with time intervals ranging from 30 minutes to 6 months. Detection of variable stars on a large range of time scales is thus also a by-product of the Hipparcos and Tycho experiments.

Duplicity is another useful information quoted in the Tycho catalog. At last useful cross-identification flags with Hipparcos and other catalogs (PPM, HD, GCVS. . .) are also mentioned.

3. The *RASS - Tycho* & *RASS - Hipparcos* samples

3.1. Construction and definition of the RasTyc and RasHip samples

The cross-correlation procedure consisted in searching for Tycho stars within 2 arcmin of each of the ≈ 150 000 X-ray sources of the RASS source list. The output data file of the correlation process between these two catalogs resulted in 38 324 entries among which 6 090 X-ray sources are associated with several (up to 20) Tycho entries. The distribution of the X-ray/Optical offset position (Dxo) for the 32 234 closest matches is shown in Fig. 1. Their number per offset bin first increases and then decreases down to a background level suggesting the obvious interpretation of the peak as those corresponding to objects which are to be physically matched in both catalogs, while the background is ascribed to spurious identifications. The histogram is well peaked around 6–7 arcsec which is known as the uncertainty affecting X-ray positions. This is due for one part to the error on the knowledge of the satellite attitude for each photon collected in scan mode and for an other part to the uncertainty with which the centroid of the X-ray image is positioned on the pixel grid by the maximum likelihood source detection algorithm.

The total number of spurious matches is related to the surface density of both the RASS and Tycho catalogs. In order to estimate the Dxo distribution of the spurious population, we computed the cross-correlation of about 150 000 positions distributed uniformly over the sky (simulating the RASS source list) with an artificial catalog simulated in a square degree around each X-ray position. The stellar density of the target catalog simulating the Tycho gradient density was 43 stars/deg^2 at low galactic latitude ($|b| \leq 20°$) and 17 stars/deg^2 at high latitude ($|b| > 20°$), corresponding to a mean surface density of 25.84/deg^2 very close to the one of Tycho. The mean Dxo distribution of the closest matches for 20 experiments is over-plotted as the grey-shaded area in Fig. 1. It is noticeable that the simulation perfectly reproduces the shape of the observed distribution above 2 arcmin. We are thus confident that the simulation gives a very good approximation of the number of spurious matches as a function of X-ray to optical distance.

Next we fitted a log normal to the distribution of *physical* matches (i.e. the total histogram minus the mean distribution of the spurious population). The best fit is over-plotted as the solid curve in Fig. 1. Results are quoted in Table 1 were we print as a function of Dxo the number of matches as well as the fraction of *physical* and *spurious* stellar X-ray sources in the sample. For an offset position Dxo = 40 arcsec the number of sources in the sample is very close to 15 667, the theoretical number of sources computed as the integral of the analytical log normal curve. On the other hand, the fraction of spurious sources at this cutoff offset distance is close to 10%. Finally we decided to define the *RASS - Tycho* sample (hereafter RasTyc) as the 13 875 matches with Dxo $\leq$ 30 arcsec, thus reducing the fraction of the spurious population to a level of about 7%. We emphasize that *RasTyc is the largest sample of stellar X-ray sources with homogeneous and accurate data constructed so far*.

For 4 984 and 722 RASS entries we found respectively 2 and 3 Tycho stars within 2 arcmin of the X-ray position. Fig. 2 shows the Dxo distributions of these second (D2) and third (D3) closest stars. While D3 shows the characteristic distribution of spurious matches, D2 shows in addition a clear excess below Dxo = 40 peaked around 10–12 arcsec. A fraction of the excess could be due to young stars in double systems, both members being X-ray emitters but the limited resolution of ROSAT preventing to

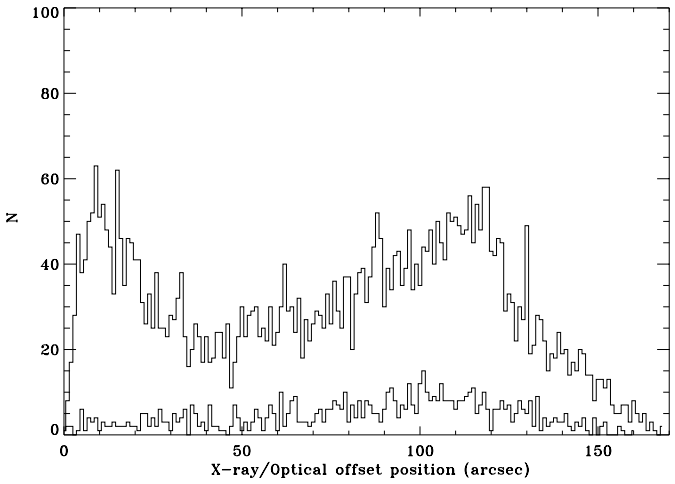

Fig. 2. Distribution of X-ray/Optical offset position (arcsec) for the 4 984 and 722 second (D2) and third (D3) closest RasTyc matches respectively. In contrast to D3 which shows a typical behavior of casual matches, D2 displays a clear enhancement below 30 arcsec (1 117 cases) probably due to double counterparts and to stars clustering.

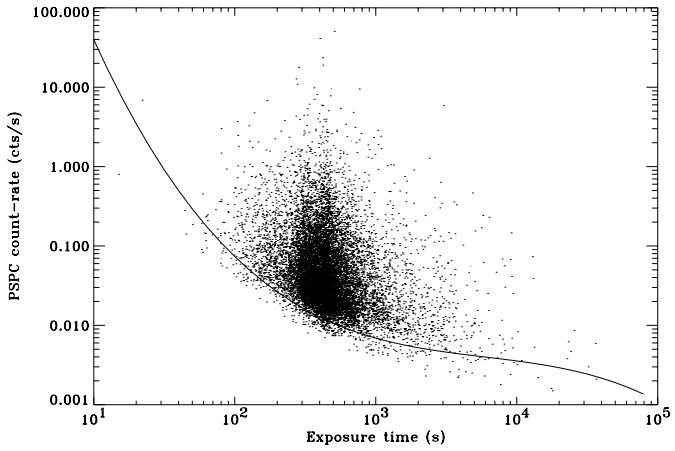

Fig. 3. ROSAT PSPC count-rate versus exposure time for the 13 875 stellar X-ray sources of the RasTyc sample. The full line is the polynomial function fitted to the lower envelope of the detections and arbitrarily shifted 0.1 dex at higher count-rate to account for the X-ray detection dependence with the background. Most of the RasTyc sources are detected in regions of the sky with exposure time between 300 and 600 s. Very faint sources (< 0.01 cts s^{-1}) are detectable only in the longer exposed regions (ecliptic poles).

detect them individually. Another fraction is probably due to detection of stars in young clusters where the surface density is significantly higher than the mean Tycho density.

Hipparcos being a sub-sample of Tycho, the RASS-Tycho matching procedure also consisted in a RASS-Hipparcos cross-correlation. We define the *RASS - Hipparcos* sample (hereafter RasHip) as the 6 200 RasTyc stellar X-ray sources also having an entry in the Hipparcos catalog. Compared to RasTyc, RasHip provides us with data about 10 times more accurate but on the other hand is reduced to 45% of the former sample. The power of the RasTyc sample is also that both RASS and Tycho observations were not based on an *a priori* observing list. Thus the RasTyc sample is only affected by well known X-ray and optical bias while RasHip, based on the *Hipparcos Input Catalog*, is affected by additional selection effects which may complicate the interpretation.

3.2. The X-ray bias

In Fig. 3 we present the PSPC count-rate of the RasTyc stars plotted versus the exposure time, all our stellar X-ray sources being detected between 50 and 0.001 cts s^{-1}. This plot perfectly demonstrates the relation between the minimum detectable count-rate S_{thr} and the exposure time t. The largest is t, the lowest is S_{thr}. This behavior introduces a position dependent X-ray bias in the RasTyc/RasHip samples: an artificial enhancement of stellar surface density towards the longer exposed regions (a striking feature at the ecliptic poles where the exposure time exceeds 1 Ksec) with respect to the shorter exposed ones.

We used Fig. 3 to derive the equation of $S_{thr} = \mathrm{f}(t)$. A polynomial was first fitted to the lower envelope of the points and then arbitrarily shifted 0.1 dex at higher count-rate. This shift is necessary to account for the dependence of detection with background. Table 2 gives the minimum exposure time needed to detect a source as faint as S_{thr} as well as the fraction of the RASS sky affected by the exposure bias at the corresponding threshold. $S_{thr} = 0.03$ cts s^{-1} appears as a good compromise to have a large sample (8 593 RasTyc and 4 422 RasHip stars) distributed over the whole celestial sphere and not heavily biased.

Table 2. Minimum exposure time required to detect stellar X-ray sources at a PSPC count rate threshold S_{thr}. P_{bias} is the fraction of the RASS celestial sphere with exposure time smaller than t.

S_{thr} (cts s^{-1})	t (s)	P_{bias} (%)
0.10	85	2
0.05	130	4
0.03	185	8
0.02	260	15
0.01	570	80

3.3. The optical bias

We present in Fig. 4 the color distribution of the 13 478 RasTyc stars with both B_T and V_T measurements (97% of the sample). The B - V Johnson color index was computed from the Tycho magnitudes according to the simple linear transformation $(\mathrm{B}-\mathrm{V})_J = 0.85\,(\mathrm{B}_T - \mathrm{V}_T)$ given in the *introduction and guide to the data* of the Hipparcos and Tycho catalogs (ESA 1997, vol.1). Compared with the whole Tycho catalog (see Fig. 2a of Høg 1997), the B - V color distribution of the RasTyc sample shows two major differences: first a very sharp decrease of the histogram in the blue part of the diagram (for B - V ≤ 0.35) and second a less prominent giants feature, only the blue part of the "clump" being visible. These main differences which are related to the X-ray emission level of stars are discussed in more details in Sect. 4. Also note that except for the paucity of blue RasTyc

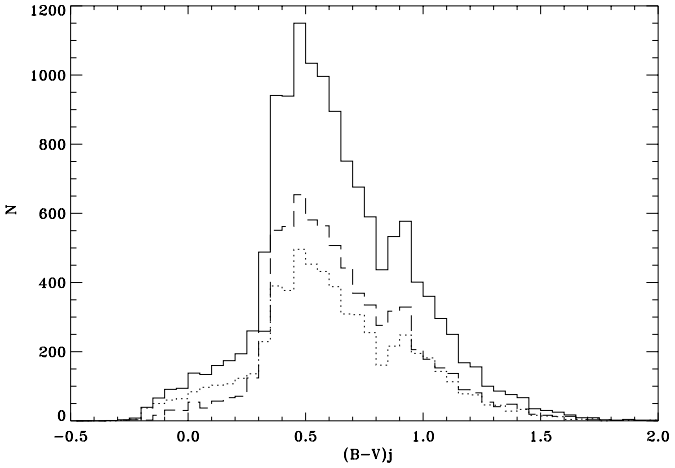

Fig. 4. B - V color index distribution in the Johnson system derived from the observed B_T and V_T magnitudes of the 13 875 RasTyc stars. The dashed and dotted histograms are computed for high ($|b| > 20°$) and low ($|b| \leq 20°$) galactic latitude respectively.

stars above $b > 20°$, the low (dotted) and high (dashed) galactic latitude histograms are very similar.

Fig. 4 also perfectly reveals the optical bias of the RasTyc sample. Because in zeroth order X-ray luminosity is color independent, young M-type stars are basically detected in the RASS up to distances at which young F-type stars can be detected too. However, the limited Tycho sensitivity excludes such optically faint stars located at large distances, implying that the RasTyc sample is more incomplete for K-M stars relative to F-G ones. This bias explains why the red peak at B - V = 1.5 observed in volume limited or X-ray flux limited sample (Sciortino et al. 1995, Motch et al. 1997) and predicted by stellar X-ray population models (Sciortino et al. 1995, Guillout 1996, Guillout et al. 1996a) is absent in the RasTyc sample.

4. Stellar X-ray emission

In this section we investigate the stellar X-ray emission throughout the HR diagram as seen from the RasHip sample. In the following we restrict to stars with accurate parallaxes ($\sigma_\pi/\pi \leq 0.1$) and color ($\sigma_{B-V} \leq 0.025$). The numbers of Hipparcos and RasHip stars satisfying these criterion are respectively 19 350 (among 118 218 i.e. 16.4%) and 3 407 (among 6 200 i.e. 55%), corresponding to a formal detection rate of 17.6%. In both samples, about 90% of the stars are brighter than magnitude 9. With a median precision of parallax for $H_p < 9$ mag of 1 mas (Perryman et al. 1997), our very stringent selection criteria $\sigma_\pi/\pi \leq 0.1$ imply that most of the stars selected are located within 100 pc of the Sun. More precisely the mean distances are respectively 73 pc ($1\,\sigma = 35$) and 58 pc ($1\,\sigma = 31$) for the Hipparcos and RasHip sub-samples respectively. It is important to note that, because the Hipparcos catalog is largely complete to around 8–9 mag (depending on galactic latitude and spectral type), *the RasHip sub-sample defined above is, as RasTyc, a stellar X-ray selected sample statistically identified with a roughly magnitude limited optical catalog*.

4.1. The X-ray selected HR diagram

In Fig. 5 we compare qualitatively the HR diagram of the Hipparcos stars *with* (b): right panel) and *without* (a): left panel) X-ray selection. Because most of the stars discussed here lie within 100 pc of the Sun no correction for interstellar extinction has been introduced. Absolute magnitudes have been therefore computed as Mv = V + 5 log(π) + 5. The B - V index corresponds to the Johnson color listed in the Hipparcos catalog. Fig. 5a is plotted for purpose of comparison only. We refer to Perryman et al. (1995) who discussed the Hipparcos HR diagram with the same astrometric and photometric selection criteria adopted here but on the preliminary solution H30.

First we note that Fig. 5b fully confirms the quasi-universality of stellar X-ray emission throughout the HR diagram discovered eighteen years ago by Vaiana et al. (1981, see their Fig. 1) from a sample of 143 stellar counterparts of Einstein X-ray sources (see also Fig. 4 of Micela et al. 1997). Fig. 5b shows a well defined Main Sequence (MS) extending from very hot (around spectral type B0) to very cool (around M5-6) objects. At a given color index, an additional scatter (0.75 mag) likely attributable to unresolved binaries and possibly to very young stars is clearly visible. Stars in the Giant branch extending from B - V $\approx$ 0.7 towards the cooler and brighter part of the diagram are also detected as X-ray sources. The distinct group of objects within the Giant branch known as the "clump" (around B - V = 1.0, Mv = 1.0) clearly shows up.

Compared with the non X-ray selected sample, Fig. 5b shows a thinner MS (0.4 mag scatter) compatible with $\sigma_{Mv} \leq 0.2$ and located very close to the theoretical Zero Age Main Sequence (ZAMS) isochrone over plotted as the thick full line. This is especially noticeable in the 0.5 - 1.0 B - V range, outside the MS turnoff which is responsible for the prominent kink in the blueward upper envelope of the MS at about B - V = 0.4, Mv = 2.5. We thus confirm the conclusion of Perryman et al. (1995) that the width of the MS in the non X-ray selected sample is attributable to intrinsic dispersion due primarily to age and evolutionary effects above B - V = 0.8. The lack of detection in the A-type stars and late-type giants regions of the HR diagram, already mentioned on the basis of the RasTyc sample B - V distribution (Sect. 3.3), is another major difference between Fig. 5a and b. Last we note that none (within the uncertainty of the statistical identification process and ZAMS position) of the subdwarfs are detected in X-ray, in agreement with what is expected for evolved stars because of the decrease of X-ray emission with age.

4.2. Detection rate

In the following subsections we discuss quantitatively the X-ray detection rate $DR = N_{RasHip}/N_{Hip}$ among the 19 350 Hipparcos stars with accurate parallaxe and color. As a consequence of the optical bias the number of Hipparcos stars per constant B - V bin decreases towards redder stars. We preferred to compute DR(B - V) so that N_{RasHip}(B - V) = 100 (except for the two last bins where this number is reduced to $\approx$ 60 and 30 respectively)

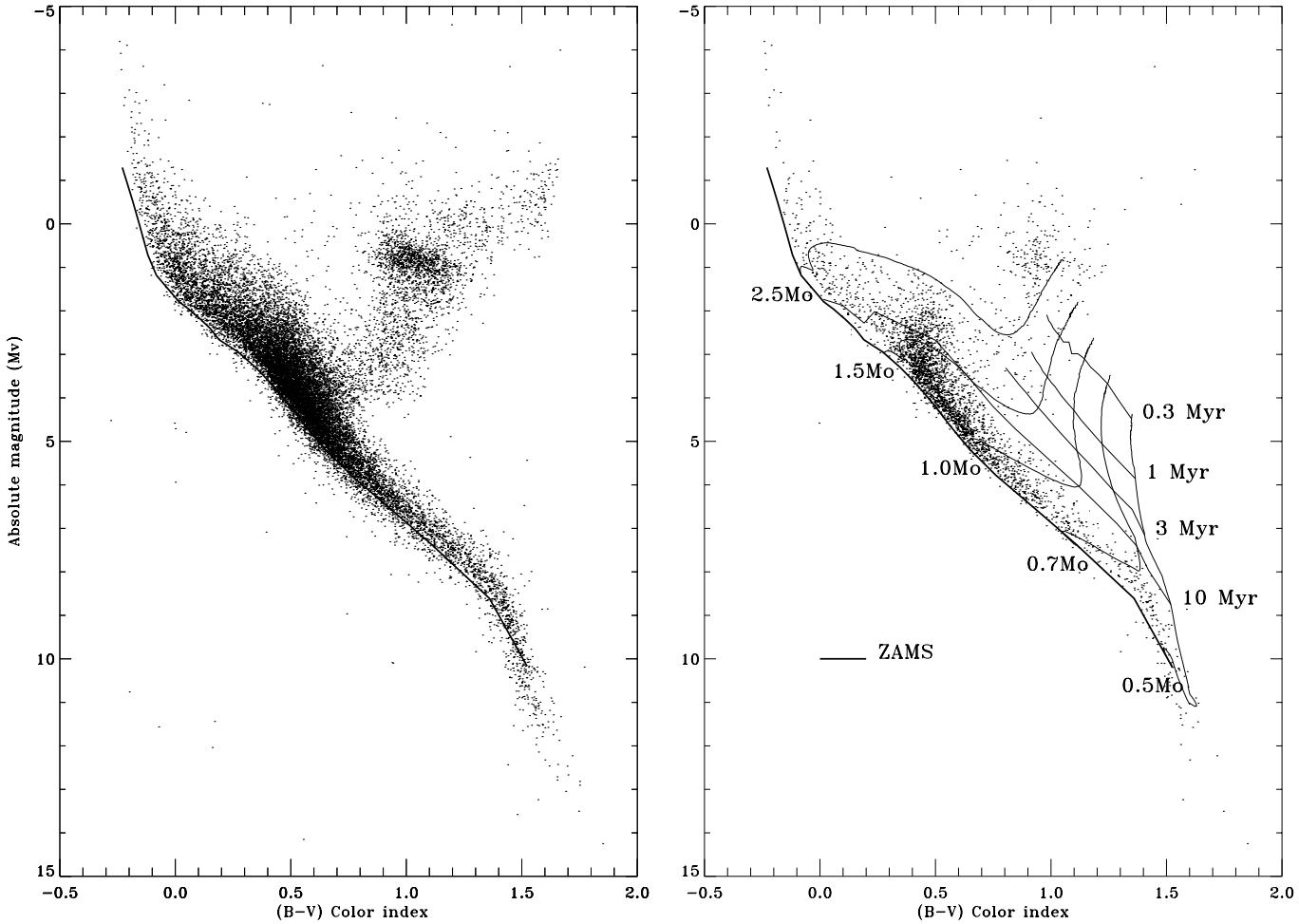

Fig. 5a and b. Observational HR diagram of the 19 350 Hipparcos (**a**: left panel) and 3 407 RasHip (**b**: right panel) stars with accurate distance ($\sigma_\pi/\pi \leq 0.1$) and color ($\sigma_{B-V} \leq 0.025$). Siess et al. (1997) PMS evolutionary tracks (from 0.5 to 2.5 $M_\odot$), isochrones (from 0.3 to 10 Myr) and ZAMS are over plotted in panel **b** (ZAMS is also plotted in panel **a**).

in order to retain an error per color bin close to 2-3%. DR is computed independently for "*on* main sequence" (roughly class V, Sect. 4.2.1) and "*off* main sequence" (roughly class III, Sect. 4.2.2) HR diagram regions. By "*on* main sequence" we mean stars located between Mv_{ZAMS} and Mv_{ZAMS} - 1.35 (at a given color) while "*off* main sequence" refers to stars located above this limit. This offset of 1.35 mag roughly corresponds to the terminal age main sequence (see Sect. 4.4). For a given color bin, DR has a meaning only if it is computed in a volume of radius $Rmax$, defined in such a way that the X-ray sample is statistically indistinguishable from the optical parent population. To test the spatial uniformity of our samples we applied the V/V_{max} method originally developed for quasars by Schmidt (1968) and generalysed by Avni & Bachall (1980). For a sample of N stars randomly distributed within a sphere of radius R_{max} (corresponding volume V_{max}), the quantity $< V/V_{max} >$ is Poisson distributed with $< V/V_{max} > = 0.5 \pm 1/\sqrt{(12 \times N)}$. We carried out the method for each sample in each B - V bin with a step of 5 pc and considered a uniform distribution until $< V/V_{max} >$ goes below $3\,\sigma$ uncertainties. Among the two R_{max} values (optical and X-ray sample) we retained the minimum one to define the sphere radius within which we computed DR. This procedure ensure that the X-ray adequaly samples the optical population. We illustrate this method in Fig. 6 for the X-ray and optical samples in two B - V ranges.

4.2.1. *On* main sequence region

In Fig. 7 upper left panel we plot as a solid line the detection rate DR with associated uncertainties (see also Table 3). Basically we can distinguish 3 regions: the "A type stars region" (B - V $\leq$ 0.33) where DR hardly exceeds 10%, the "F type stars region" ($0.33 < B - V \leq 0.54$) where DR peaks around 35% and the "G-M region" where DR increases from 15% (at B - V = 0.55) up to about 45% (at B - V = 1.5).

Since the beginning of stellar X-ray astronomy X-ray emission from A-type stars has been a subject of debate, these stars being not convincingly detected. Although some RASS sources match A-type stars, DR is significantly lower (by a factor > 2) than for F-M type stars, a feature already noticed for the RasTyc sample on the basis of the B - V distribution (see Sect. 3.3). From a theoretical point of view this corresponds to the disappearance

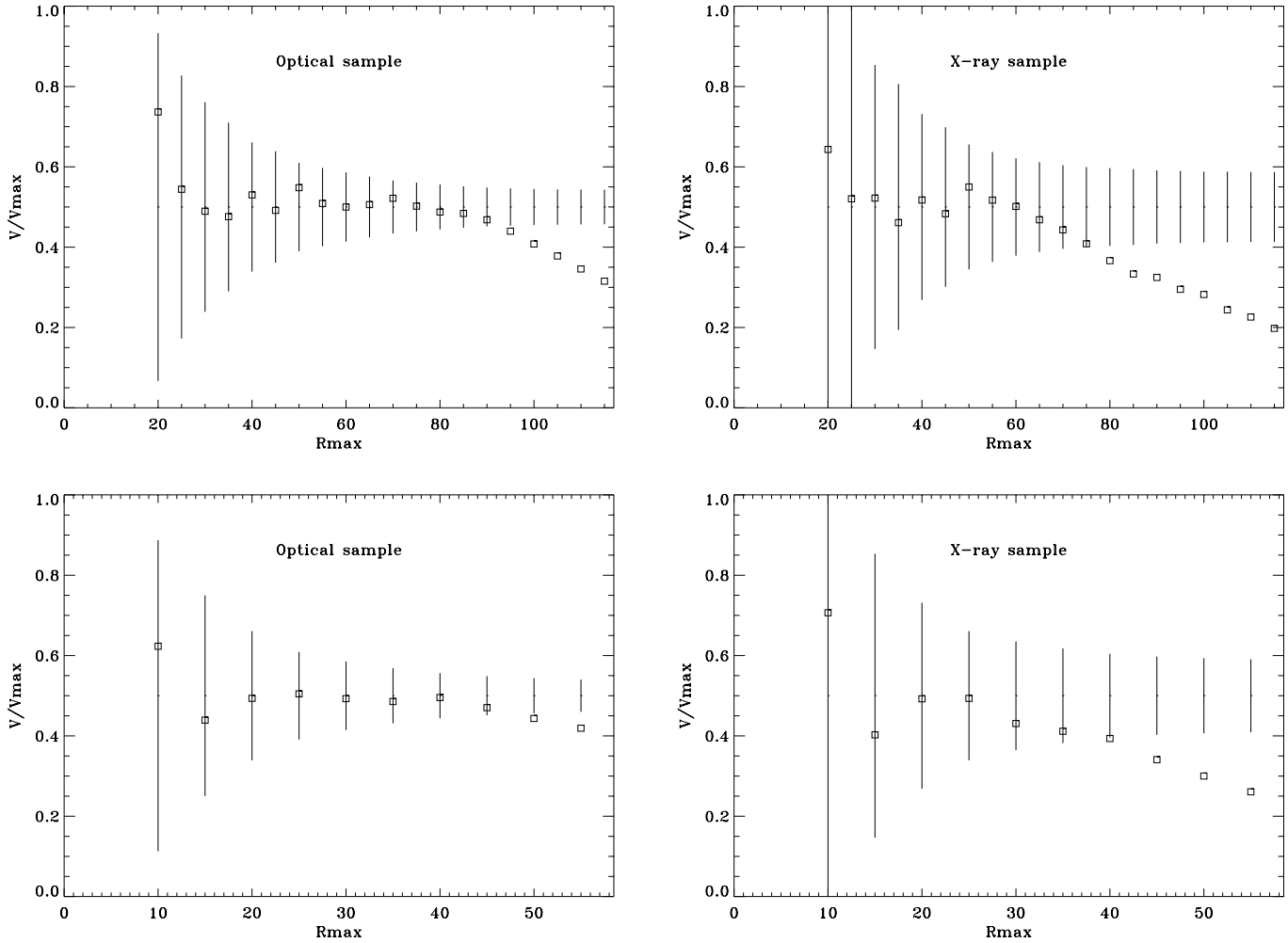

Fig. 6. $< V/V_{max} >$ (square symbols) versus $Rmax$ in case of $0.46 < B - V \leq 0.47$ (upper panel) and $0.76 < B - V \leq 0.83$ (lower panel) for the optical (left side) and X-ray (right side) samples. The $3\,\sigma$ uncertainties (vertical bar) in the hypothesis of stars randomly distributed within Vmax (corresponding to sphere of radius Rmax) is also plotted.

of subsurface convection zones. According to dynamo theory, a source of non radiative energy is required to heat the coronae and when this energy is no longer available X-ray emission stops. Thus A-type star X-ray emission is generally attributed to a low-mass companion or to an unrelated neighboring star (Schmitt et al. 1985, Schmitt 1992, Simon & Drake 1993, Simon et al. 1995). The drop of detection rate for A-type stars can be considered as an observational test of internal structure and dynamo theories. According to Bohn (1984), the internal structure transition should occur for an effective temperature of 8 500 K corresponding to an A3 main sequence type while our observed cut occurs at A9-F0. For B - V < 0, DR increases to $\approx$ 15% as we move in a region of the HR diagram where stellar effective temperatures are sufficiently high for radiatively driven winds (as in the X-ray emitting O and early-B stars).

For main sequence F-M type stars, the internal structure permits the dynamo mechanism (required to heat the coronae) to operate and these stars are convincingly detected as X-ray sources.It is known that the Fx/Fopt ratio increases with decreasing effective temperature (Schmitt 1990). This is illustrated from our data in Fig. 7 middle left panel where we plot the logarithm of Fx/Fopt (see also Table 3) computed as log(PSPC count rate) + V/2.5 - 5.63 following the expression used by Maccacaro et al. (1982) and assuming an average energy conversion factor of 1 PSPC cts s^{-1} for a 10^{-11} erg cm^{-2} s^{-1} flux in the range 0.1 to 2.4 keV. The color dependence of this ratio introduces a bias in X-ray and magnitude limited sample which favors the detection rate for cooler stars. In order to take this bias into account we computed for each bin a *corrected detection rate normalized to the one in the last bin* i.e. $DR_c = < Fx/Fopt >_{last} / < Fx/Fopt > \times DR / DR_{last}$. $DR_c > 1$ thus means that the detection rate corrected for Fx/Fopt bias is larger that the one computed in the last bin (i.e relative to M type stars). DR_c is over plotted as the dash-3dots curve in Fig. 7 upper left panel. Once corrected for Fx/Fopt bias the detection rate is remarkably constant for G-M stars ($0.54 < B - V \leq 1.5$) as expected. On the other hand the correction factor enhances the peak of detection for F-type stars ($0.33 < B - V \leq 0.54$) which reaches a factor 8 with respect to G-M stars (see Table 3). Reducing the off main sequence

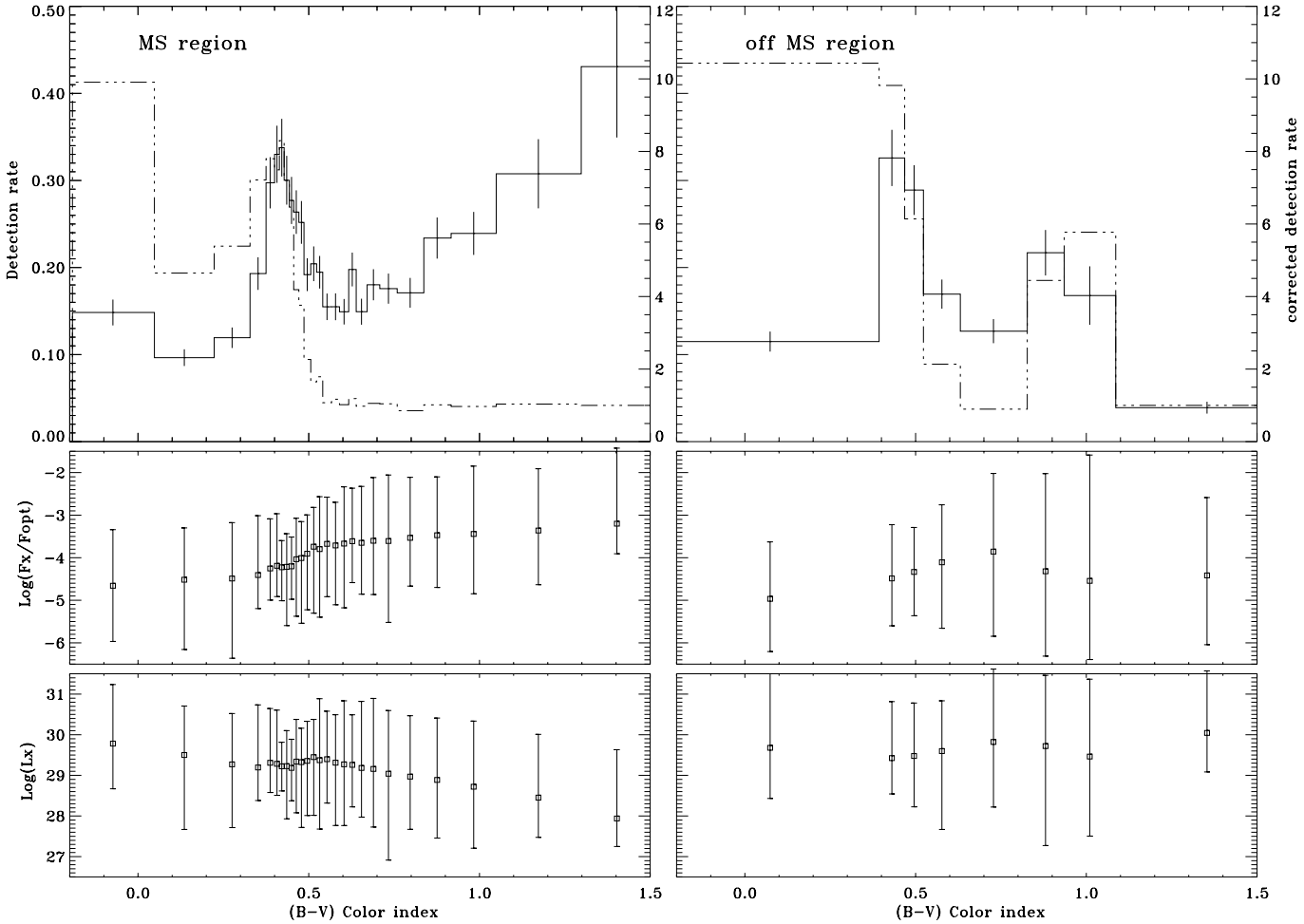

Fig. 7. Detection rate (solid line, upper panel) and associated errors for Hipparcos stars with accurate parallaxe and color. Corrected detection rate is over plotted as the dash-3dots line scaled according to right of the graph. We also show logarithm of the mean Fx/Fopt ratio (middle panel) and X-ray luminosity (lower panel) for those stars detected as X-ray sources (with associated min-max values plotted as the vertical bars). Computations are done as a function of B - V color index for "*on* main sequence" (left panel) and "*off* main sequence" (right panel) regions. See text for details.

offset (see Sect. 4.2) from 1.35 to 0.75 mag reveals exactly the same behavior. This indicates that these features are intrinsic to MS stars and are not due to contamination by evolved stars which show similar behavior (see Sect. 4.2.2).

Two effects could lead to higher detection rates for F-type stars in the RasHip sub-sample. First, according to evolutionary models (Siess et al. 1997), the main sequence life time decreases from 9.5 Gyrs for 1 $M_\odot$ stars (i.e. G2) to about 1.5 Gyrs for 1.6 $M_\odot$ stars (i.e. F0). Thus, on the average, the "G-M *On* main sequence" Hipparcos sub-sample is intrinsically older (it's a mixture of stars from 0 to 10 Gyrs) than the "F *On* main sequence" Hipparcos sub-sample which only contains stars younger than 1.5 Gyrs (older ones being on post-MS evolutionary tracks). It is well known from X-ray observations of galactic clusters that X-ray emission decreases with age (Micela et al. 1988, 1990, Barbera et al. 1993) however stellar X-ray population models (Micela et al. 1993, Guillout et al. 1996a) predict that stars older than 1 Gyrs still account for up to 40% (at high galactic latitude). Thus DR_c is expected to be slightly higher among F-type stars than among G-M stars. Second, each V_{max} volume in which we computed the detection rate is set up either by the X-ray or by the optical sample, depending on the mean absolute magnitude of the bin (see Sect. 4.2). As an X-ray flux limited sample does contain a higher fraction of young stars compared to an optically limited one and because this transition occurs around B - V = 0.5, we again expect a better detection rate among F-type stars than among G-M stars. While these two effects certainly play a role, they are unlikely to account for a factor 8 increase of DR_c.

Roughly, F-type stars mark the transition between rapid rotators with thin convective envelope and slow rotators with thick convective ones. The amplitude of variation of DR_c over a very small B - V range tends to prove that the heating of the coronae is an extremely sensitive mechanism and may indicate that both internal structure (i.e. depth of convection zone) and physical properties (i.e. rotation rate) encountered for main sequence F-type stars strongly favor the efficiency of the dynamo. We also note that the mean X-ray luminosity which increases from M

Table 3. Detection rate DR (%), mean Fx/Fopt ratio plus minimum (indices) and maximum (index) values, Fx/Fopt corrected detection rate DR_c (relative to last bin) and mean X-ray luminosity plus minimum (indices) and maximum (index) values computed as a function of B - V in case of *On* main sequence region (see text for details)

B-V range	DR	log(Fx/Fopt)	DR_c	log(Lx)
-0.192 0.045	14.84	$-4.66^{-3.34}_{-5.97}$	9.91	$29.78^{31.24}_{28.67}$
0.048 0.223	9.65	$-4.52^{-3.30}_{-6.16}$	4.65	$29.51^{30.71}_{27.67}$
0.223 0.328	11.94	$-4.49^{-3.18}_{-6.36}$	5.39	$29.27^{30.52}_{27.71}$
0.328 0.375	19.31	$-4.41^{-3.01}_{-5.20}$	7.22	$29.18^{30.73}_{28.38}$
0.375 0.399	29.74	$-4.25^{-3.09}_{-5.00}$	7.80	$29.30^{30.64}_{28.58}$
0.400 0.414	33.01	$-4.19^{-2.97}_{-4.91}$	7.49	$29.28^{30.61}_{28.51}$
0.414 0.428	33.77	$-4.22^{-3.60}_{-5.01}$	8.30	$29.22^{29.81}_{28.62}$
0.428 0.443	30.03	$-4.21^{-3.44}_{-5.60}$	7.20	$29.22^{30.10}_{27.93}$
0.443 0.456	27.70	$-4.20^{-3.51}_{-4.98}$	6.46	$29.19^{29.89}_{28.37}$
0.456 0.471	26.37	$-4.04^{-3.07}_{-5.38}$	4.19	$29.34^{30.38}_{28.08}$
0.471 0.486	25.18	$-4.01^{-3.15}_{-5.54}$	3.76	$29.33^{30.16}_{27.72}$
0.486 0.505	19.18	$-3.91^{-2.99}_{-5.22}$	2.27	$29.35^{30.33}_{28.01}$
0.506 0.523	20.43	$-3.74^{-2.82}_{-5.30}$	1.65	$29.45^{30.38}_{28.01}$
0.523 0.541	19.46	$-3.80^{-2.57}_{-5.40}$	1.79	$29.39^{30.89}_{27.68}$
0.541 0.566	15.49	$-3.67^{-2.58}_{-4.92}$	1.07	$29.40^{30.58}_{28.32}$
0.567 0.590	15.49	$-3.71^{-2.70}_{-5.11}$	1.17	$29.31^{30.49}_{27.77}$
0.590 0.617	14.92	$-3.67^{-2.33}_{-5.18}$	1.02	$29.26^{30.84}_{27.76}$
0.617 0.638	19.77	$-3.61^{-2.37}_{-4.59}$	1.19	$29.26^{30.49}_{28.22}$
0.639 0.670	14.93	$-3.65^{-2.32}_{-4.86}$	0.98	$29.18^{30.82}_{27.97}$
0.671 0.708	18.02	$-3.60^{-2.12}_{-4.87}$	1.05	$29.15^{30.89}_{27.73}$
0.708 0.759	17.58	$-3.61^{-2.06}_{-5.52}$	1.04	$29.04^{30.60}_{26.91}$
0.759 0.835	17.09	$-3.53^{-2.11}_{-4.67}$	0.85	$28.99^{30.66}_{27.67}$
0.837 0.915	23.39	$-3.47^{-2.10}_{-4.70}$	1.01	$28.90^{30.41}_{27.46}$
0.917 1.049	23.92	$-3.44^{-1.85}_{-4.85}$	0.97	$28.77^{30.40}_{27.21}$
1.049 1.296	30.77	$-3.36^{-1.91}_{-4.63}$	1.04	$28.70^{30.13}_{27.61}$
1.298 1.507	43.08	$-3.20^{-1.43}_{-3.91}$	1.00	$28.56^{30.08}_{27.55}$

to OB stars flattens in the F-type stars region and that the Lx distribution is significantly narrower compared to other regions (see Fig. 7 lower left panel and Table 3). X-ray luminosity functions will be presented and extensively discussed in Guillout et al. 1999.

Finally we note that DR_c in the A-type star region is close to 4 i.e. intermediate between the F and G-M values as expected if a late type (F-M) young companion is responsible for the X-ray emission.

4.2.2. *Off* main sequence region

The X-ray emission of evolved stars has been largely discussed by Hünsch, Schröder and collaborators using RASS or pointed observations of a volume limited sample of class III, IV stars. Hünsch & Schröder (1996) and Schröder et al. (1998) have suggested that a direct transition of the "X-ray dividing line" (XDL, a vertical line in the HR diagram at about K3 first introduced by Ayres et al. 1981), from heating coronae (left of the XDL) to driving cool stellar winds (right of the XDL) does not take place. Rather they propose a scenario in which stellar activity decreases gradually as stars evolve along the post-MS evolutionary tracks and suggested a revised XDL coinciding approximatively with the 1.2 $M_\odot$ evolutionary track on its ascent in the red Giant branch, the initial angular momentum and the different evolutionary history (as a function of mass) naturally accounting for the XDL.

We conducted for *Off* main sequence region a similar analysis as the previous one (see Sect. 4.2.1). We plot the corresponding graphs in Fig. 7 right panels and present results in Table 4. The most striking features of Fig. 7 upper right panel are on one hand the strong detection rate in the turnoff ($DR \approx 30\%$) and "clump" ($DR \approx 22\%$) regions, and on the other hand a dramatic decreases of DR for B - V > 1.1 to a level close to 4% compatible with the fraction of spurious matches in the RasHip sample. Note that normalization to the last bin implies in this case that $DR_c \approx 1$ corresponds to no significant detection. Once corrected for Fx/Fopt bias, DR_c confirms a significant detection rate in the turnoff and the "clump" but reveals a lack of detection in the Hertzsprung gap region ($0.63 \leq B - V \leq 0.82$, $DR_c = 0.9$).

Stars located in the turnoff ($0.39 \leq B - V \leq 0.52$) have A-B type progenitors on the MS which are known to be very fast rotators. As they evolve they develop outer convection zones and consequently large degree (expected from their high rotation rate) of magnetic activity partly released as X-ray emission. These stars evolve along the post-MS evolutionary tracks and then concentrate in the blue part of the clump (as Helium burning giants) corresponding to the 0.83–1.08 B - V bins where $DR_c \approx 5$. We note that the high detection rate observed in the "K giant clump" region confirms the finding of Schröder et al. (1998) that magnetic activity survives the Helium flash.

For $0.52 \leq B - V \leq 0.83$, the dominating population consists of stars with $M_V > 3$ (see Fig. 5a) i.e. with mass $M \leq 1.1\,M_\odot$. These G-type stars have spun down during their MS life time (> 6.3 Gyrs) and are probably Sun-like X-ray bright (or fainter) which would explains the insignificant detection rate ($DR_c = 0.9$) in this region of the HR diagram as well as on the right side of the "clump" ($DR_c = 1$). These theoretical considerations naturally explain the behavior of the detection rate in the various *off* main sequence regions. We note that despite of completely different sample, these results are fully compatible with those from Hünsch, Schröder and collaborators to which we refer for additional discussion.

5. The question of the PMS population

T Tauri stars (TTS) were first recognized as a separate class of stars by Joy (1945). Almost all TTS known prior to the ROSAT launch were located in or near dark molecular clouds (usually defined by CO surveys) with ongoing star formation, i.e. close to their birthplace as expected for very young stars (*very young stars* meaning here age < 10 Myr). Spectroscopic observations in the red part of the spectrum led to the distinc-

Table 4. Detection rate DR (%), mean Fx/Fopt ratio plus minimum (indices) and maximum (index) values, Fx/Fopt corrected detection rate DR_c (relative to last bin) and mean X-ray luminosity plus minimum (indices) and maximum (index) values computed as a function of B - V in case of *Off* main sequence region (see text for details)

B-V range	DR	log(Fx/Fopt)	DR_c	log(Lx)
-0.243 0.391	11.49	$-4.97^{-3.63}_{-6.20}$	10.43	$29.68^{28.43}_{31.50}$
0.393 0.468	32.59	$-4.49^{-3.22}_{-5.60}$	9.82	$29.42^{28.54}_{30.82}$
0.468 0.523	28.90	$-4.33^{-3.29}_{-5.36}$	6.14	$29.48^{28.23}_{30.78}$
0.523 0.631	16.94	$-4.11^{-2.76}_{-5.66}$	2.14	$29.60^{27.67}_{30.83}$
0.631 0.825	12.69	$-3.86^{-2.02}_{-5.85}$	0.90	$29.82^{28.22}_{31.62}$
0.827 0.934	21.70	$-4.32^{-2.02}_{-6.31}$	4.44	$29.72^{27.27}_{31.46}$
0.935 1.085	16.78	$-4.54^{-1.59}_{-6.39}$	5.77	$29.46^{27.50}_{31.37}$
1.086 1.621	3.90	$-4.42^{-2.59}_{-6.04}$	1.00	$30.04^{29.08}_{31.57}$

tion of the so-called classical (CTTS) and weak-line (WTTS) TTS, depending on their Hα emission and Lithium absorption lines strength. TW Hya (Rucinski & Krautter 1983) and later on CoD-29°8887 (de la Reza et al. 1989) were recognized as the prototypes of the classical and weak-line *isolated* TTS. They exhibit all characteristics of TTS but are located several degrees off any remnant cloud material. More recently ground-based optical follow-up observations of RASS sources have identified a widely dispersed population of WTTS (Alcalá et al. 1995, 1996, Wichmann et al. 1997, Krautter et al. 1997). Bricẽno et al. (1997), Micela et al. (1997) and Favata et al. (1997) have cast some doubts on the nature of the widespread WTTS population, suggesting that a fraction is likely to be Pleiades-like main sequence stars. Finally in the light of new high resolution spectroscopic observations, Covino et al. (1997) confirm the existence of very young stars far from the main Chamaeleon cloud as well as a foreground Pleiades-like population which contaminates their original sample. It has become increasingly evident during the last two years that a considerable number of very young stars is present in the solar neighborhood, which are unrelated to prominent star forming regions. As stellar activity decreases with increasing age, it can serve as a proxy age indicator. With respect to chromospheric activity, Henry et al. (1996) published the results of a Ca II H and K emission strength survey for 800 solar-type, southern stars in the solar neighborhood. Their subsample of "very active" stars indeed contains a large fraction of young ($\leq$ 100 Myr) stars. Their youth is confirmed by the presence of high abundances of photospheric lithium found with high-resolution optical spectroscopy (Soderblom et al. 1998). Also the coronal activity of those nearby field stars from the Gliese catalog that are detected in the RASS were analyzed by Sterzik & Schmitt (1997). The coronally most active stars contain a certain fraction of apparently very young stars, as inferred from their lithium abundances. More very young stars are suspected in the solar neighborhood based on other features such as IR excess, and characteristic kinematics (Jeffries 1995).

The existence of very young stars far from interstellar material is difficult to reconcile with the standard scenario of star formation. They are too young to have travelled the distance from the nearest clouds in their short life time if one assumes the canonical velocity dispersion (1–2 km s^{-1}) observed in star forming regions. Different scenarios have been proposed as possible explanation for the presence of TTS far away from molecular clouds. Sterzik et al. (1995) suggested that isolated Pre Main Sequence (PMS) stars have been ejected (*run-away* TTS) from their birth place in favor of close encounters with other members of their parent cloud (see also Sterzik & Durisen 1995). Alternatively they may have form locally from small cloud as suggested by Feigelson (1996).

If isolated TTS are common in the Galaxy (or at least in that region of the Galaxy), a fraction of them should be present in the RasTyc and RasHip sample. As a consequence of their youth, they have to be located well above the MS in the HR diagram. As mentioned at the beginning of Sect. 4 most of the stars in the RasHip sub-sample are located within 100 pc of the Sun, i.e physically several tens of parsec away from the closest ongoing star forming regions (the Taurus-Auriga and Ophicius-Scorpius Lupus-Centaurus complex). The RasHip sub-sample offers the opportunity to address this question with the aim to derive an upper limit to the fraction of isolated TTS in the solar neighborhood.

In Fig. 5b we overplot the PMS evolutionary tracks for solar abundances (from 0.5 to 2.5 $M_\odot$), isochrones (from 0.3 to 10 Myr) and ZAMS from the new evolutionary models of Siess et al. (1997). We used T_{eff}-color and T_{eff}-BC calibrations tabulated in their Table 1 to transform the theoretical (log(L), log(T_{eff})) diagram to the observational (Mv, B - V) one. It is noticeable that the theoretical ZAMS perfectly fits the lower envelope of the observed RasHip sub-sample HR diagram except for B - V $>$ 1.3 where both models and calibrations are subject to large errors. Note that we would have obtained similar results with other evolutionary tracks (see Siess et al. (1997) for comparison with D'Antona & Mazzitelli and Swenson et al. models).

It is useful to recall that during their MS life time stars in the HR diagram move along the so called MS evolutionary tracks to reach the Terminal Age Main Sequence (TAMS). This evolution is partly responsible of the 1 to 2 mag width of the MS seen in Fig. 5a (see Sect. 4.1). Then stars leave the MS to the Giant branch, evolving along the post-main sequence evolutionary tracks. From a theoretical point of view, depending on the position in the HR diagram, one can have different evolutionary status. For example, a star located in the blue kink near B - V = 0.4, Mv = 2.5 can be interpreted as a 2.0 $M_\odot$ 10 Myr star evolving along the PMS radiative tracks towards the ZAMS, as well as a 1.6 $M_\odot$ 1 Gyr one in its MS phase or even as a 1.7 $M_\odot$ 2 Gyr old star leaving the TAMS. To largely overcome these drawbacks we restrict in the following to the 364 RasHip stars of Fig. 5b with $0.6 < B - V < 0.7$ and Mv $\geq$ 3.0 thus avoiding most of the giants which M $>$ 1.3 $M_\odot$ post-main sequence evolutionary tracks (not plotted) are brighter than the adopted Mv. In this B - V range, the TAMS can be approximated by M_{TAMS} = 6.3 (B - V) + 0.4 (see Fig. 4 of Siess et al. 1997).

5.1. Multiplicity

In the range of color and absolute magnitude defined above 247 (67.8%) stars among the 364 selected lie between the ZAMS and the TAMS. From the theoretical point of view these stars are at minimum 20 to 30 Myr old, most of them probably being ZAMS or older. Those 117 (32.2%) stars located above the TAMS could be double or multiple systems unresolved by Hipparcos and/or PMS objects (see next subsection). In order to roughly address these questions we checked for additional informations in the SIMBAD database. For 64 out of 117, nothing is known with regards to duplicity or evolutionary status. For the remaining 53 stars, 17 (32%) are spectroscopic binaries, 30 (57%) are members of double or multiple systems (which could explain the *off* MS position) and 6 (11%) are mentioned as giant or subgiant. These additional pieces of information are insufficient to draw quantitative conclusions concerning the contribution of binaries to the *above* MS population but show that as expected, binarity/multiplicity play a fundamental role. Note the small contribution of evolved stars partly due to our choice of the HR diagram region.

5.2. Isolated TTS

T-Tauri stars in ongoing star forming regions (Alcalá et al. 1995, 1996, Wichmann et al. 1996, Krautter et al. 1997, Covino et al. 1997) have been the subject of many studies with the RASS data or dedicated pointing observations. These studies indicate that WTTS are strong X-ray emitters with X-ray luminosity $\mathrm{Lx} = 10^{30.0 \pm 0.5}$ erg s^{-1}. According to Wichmann et al. (1996) and Neuhäuser et al. (1997), 70% to 80% of the newly discovered WTTS detected during the ROSAT All-Sky Survey in and around star forming regions have X-ray luminosity larger than $\mathrm{Lx}_{TT} = 10^{29.8}$ erg s^{-1}. We used this constrain on Lx as an additional parameter to infer the fraction of possible PMS stars far from any star forming region in the RasHip sub-sample.

Among our 364 stars only 27 (7.4%) are X-ray bright ($\mathrm{Lx} \geq \mathrm{Lx}_{TT}$) and located above the TAMS, the two conditions to be retained as possible *isolated* TTS. In order to improve statistics we extended our B - V range down to 0.8. Among the 566 stars now selected, 369 (65.2%) are compatible with the MS and 45 (7.9%) out of those 197 (34.8%) located above the TAMS, are also X-ray bright. Note that the fraction of MS, *off* MS and possible *isolated* TTS are the same (within a few percent) as in the case of the smaller B - V range. The SIMBAD database reveals that among the 45 stars retained, 20 are RS Cvn or BY Dra systems, 8 are spectroscopic binaries, 1 is member of the IC1396 cluster and 4 are members of double or multiple systems. Note that according to the definition of RS Cvn and BY Dra, these 8 very active spectroscopic binaries can be considered as new members of these class of stars. We are left with 12 stars for which nearly nothing is known and which fill our criterion for isolated TTS candidates (i.e. above the TAMS and $\mathrm{Lx} \geq 10^{29.8}$ erg s^{-1}). Their location in the HR diagram implies ages between 5 and 30 Myr but high resolution spectroscopic observations are necessary to single out spectroscopic binaries and to conclude on their PMS nature by mean of their H_α emission and Li absorption, a combination that is characteristic of TTS.

Even if none of them reveals to be giant or spectroscopic binary the fraction of isolated TTS in the RasHip sub-sample would hardly reach 2–3%. However we emphasize that this fraction would statistically imply hundreds of isolated TTS in the solar neighborhood (72 among the 3 407 RasHip stars with accurate distance and color and ≈ 300 for the whole RasTyc sample). If no dark clouds that might have supplied the material for the star formation can be identified around their position, these stars would be new pieces to the pulzzing question of the presence of very young objects far away from molecular clouds. Finally we note that given their age and proximity, these stars would allow to give new insight into the process of planets formation.

6. Probing galactic structure and evolution parameters with the RasTyc and RasHip samples

The cross-correlation of the RASS with the Tycho/Hipparcos catalogs provided us with an unprecedented amount of stellar X-ray sources with accurate X-ray and optical data. In the following we briefly discuss the pending questions where the RasTyc and/or RasHip samples are likely to give new insight.

The large-scale distribution of young stars in the solar neighborhood is an important question that can be address by the RasTyc/RasHip samples. In addition to the scale height of young stars, detailed investigations of the RasTyc stellar surface density by Guillout et al. (1998a,b) reveal a noticeable asymmetry with respect to the galactic plane. Interpreting the observed density enhancement as a coherent feature they derived an inclination $i = 27.5^\circ$ and an ascending node $\mathrm{l}_\Omega = 282^\circ$ with respect to the galactic plane. Both values are very close to those quoted in the literature for the Gould belt (hereafter GB, Gould 1879, Pöppel 1997 and reference therein) and in fact consistent with them. Detailed analysis of the surface density, distance and X-ray luminosity distributions led them to introduce a slightly modified scenario (namely *Gould disk*) in which the GB is not a "belt" but rather a disk composed of young stars, disrupted near the Sun. This scenario is suitable to explain the wide radial distance distribution observed for GB late-type stars in excess of the ambient galactic plane population. Guillout & Sterzik (1999) show that depending on its orientation and position the GB could provide an alternative explanation for the presence of WTTS widely distributed around star forming regions (depending on their position) and also may explain the presence of isolated very young stars.

Star formation rate (SFR): Constraining the SFR is the most straightforward result that can be achieved by comparing stellar X-ray population model number count predictions with observations (Micela et al. 1993, Guillout 1996, Guillout et al. 1996b). However, the reduced size of the sample (generally restricted to less than a few 100 deg^2) has prevented from establishing severe constraints because of low statistics. The entire sky coverage at the RASS sensitivity of the RasTyc sample is perfect for this study.

Initial mass function below 1 $M_\odot$ (IMF): Constraining the IMF requires observed color index distribution (generally B - V) to be compared with model predictions. Also the size of the sample must be sufficiently large to retain acceptable statistics after bining. With its 2 magnitudes B_T and V_T mostly better known than ≈ 0.03 mag, the RasTyc sample will allow to address this problem.

Scale height of young stars: So far, this parameter is poorly known because of the difficulties encountered to properly select young main sequence late type stars (F-M). On the other hand efficient selection of such stars using X-ray data will allow to overcome the problem. Thus, the observed distribution of X-ray active stars can be used to constrain the scale height of the youngest population and indeed the analysis by Guillout et al. (1998a) of the stellar surface density of the 8 593 RasTyc stars detected at a PSPC count-rate threshold $S = 0.03\,\mathrm{cts\,s^{-1}}$ (see their Fig. 3) shows the expected gradual decrease from low to high galactic latitude.

Dynamics of young stars: For the optically brightest stars the RasTyc and RasHip samples provide accurate proper motions. Predictions of the *Besançon X-ray population model* (Guillout et al. 1996a) include kinematical outputs such as radial velocity, proper motions and true motions. Comparison of such outputs with observations may address the question of the thermalization of this young population and the shape of the age velocity dispersion relation (related to a process known as "disk heating").

7. Conclusions and perspectives

The cross-correlation of the RASS with the Tycho/Hipparcos catalogs provided us with the largest samples of stellar X-ray sources statistically identified so far, the so-called RasTyc and RasHip samples. This drastically improved the quality of the optical parameters and also supplied homogeneous parallaxes and accurate proper motions for X-ray sources successfully cross-correlated with stars. The RasTyc and RasHip samples are affected by well understood optical and X-ray biases due to the optical and X-ray flux limited nature of the input catalogs. We presented the X-ray selected HR diagram and showed that X-ray emitting stars are detected all along the very hot (O-B stars) to very cool (M stars) main sequence. Once corrected for Fx/Fopt bias, the detection rate for F main sequence stars appears significantly higher than for G-M stars. This may indicate that the heating of the coronae is an extremely sensitive mechanism and that both internal structure and physical properties encountered for main sequence F-type stars strongly favor the efficiency of the dynamo. On the other hand for A-type stars, for which effective temperatures are too low for radiatively driven winds but too high for deep envelope convection and associated convectively driven coronae, the detection rate drops at a level compatible with those observed for F-M stars. The main sequence "turnoff" and the "K giant clump" are also prominent features of the X-ray selected HR diagram. Theoretical considerations naturally explain the observed detection rate in the various parts of the HR diagram.

We showed that, in agreement with predictions of stellar X-ray population models, most of the RasTyc/RasHip stars are ZAMS or older. We emphasize that these young stars are present in any regions of the sky and that studies discussing X-ray sources in the general direction of star forming regions must account for this ambient population otherwise they are likely to overestimate the number of WTTS, especially in large areas or deep pointings. So far the RasTyc-RasHip samples give us the most reliable estimate of this ambient Galactic plane population at the RASS limiting sensitivity. A crude analysis of the '*off* main sequence' population does not rule out the presence of isolated PMS stars in the RasTyc/RasHip samples but high resolution spectroscopic observations are needed to conclude on their PMS nature. While their fraction probably does not exceed 2–3% (upper limit), they may be as numerous as 300 in the RasTyc sample. Given their age and proximity, these stars would be perfect for studying the process of planets formation.

The RasTyc/RasHip samples are best suited to study the large scale distribution of young X-ray active stars in the solar neighborhood. In conjunction with stellar X-ray population models they are likely to give new insight on Galactic structure and evolution parameters such as the mean value of the star formation rate during the last billion years, the slope of the initial mass function at the low mass end, the scale height and the dynamical state of young stars in relation with the disk heating process.

Acknowledgements. This study is based on observations made with ROSAT and with the ESA Hipparcos astrometry satellite and makes use of the SIMBAD database maintained by CDS, Strasbourg. The ROSAT project is supported by the Bundesministerium für Bildung, Wissenschaft, Forschung und Technologie (BMBF/DLR) and the Max-Planck-Gesellschaft (MPG). P.G. acknowledges support from a CNRS-MPG cooperation. We are grateful to the Tycho Consortium for accessing the Tycho catalog in advance of publication.

References

Alcalá, J.M., Krautter, J., Schmitt, J.H.M.M., Covino, E., Wichmann, R., et al., 1995, A&AS 114, 109
Alcalá, J.M., Terranegra, L., Wichmann, R., Chavarria-K, C., Krautter, J., et al., 1996, A&AS 119, 7
Avny, Y., Bachall, J.N., 1980, ApJ 235, 694
Ayres, T.R., Linsky, J.L., Vaiana, G.S., Golub, L., Rosner, R., 1981, ApJ 250, 293
Barbera, M., Micela, G. Sciortino, S., Harnden, F.R., Rosner, R., 1993, ApJ 414, 846
Bohn, H.U., 1984, A&A 136, 338
Bricẽno, C., Hartmann, L.W., Stauffer, J.R., Gagné, M., Stern, R.A., 1997, ApJ 113, 740
Covino, E., Alcalá, J.M., Alain, S., Bouvier, J., Terranegra, L., et al., 1997, A&A 328, 187
de la Reza, R., Torres, C.A., Quast, G., Castilho, B.V., Vieira, G.L., 1989, ApJ 343, L61
Egret, D., Fabicius, C., 1997, Proceedings of the ESA symposium, ESA SP-402
ESA, 1993, The Hipparcos Input Catalogue, ESA SP-1136
ESA, 1997, The Hipparcos and Tycho Catalogues, ESA SP-1200
Favata, F., Micela, G., Sciortino, S., 1997, A&A 326, 647

Feigelson, E.D., 1996, ApJ 468, 306
Gioia, I.M., Maccacaro, T., Schild, R.E., Wolter, A., Stocke, J.T., et al., 1990, ApJS 72, 567
Gould B.A., 1879, Uranometria Argentina, ed. P.E. Corni, Buenos Aires, p. 354
Guillout, P., 1996, Thesis, Observatoire Astronomique de Strasbourg, Université Louis Pasteur, France
Guillout, P., Haywood, M., Motch, C., Robin, A.C., 1996a, A&A 316, 89
Guillout, P., Haywood, M., Motch, C., Robin, A.C., 1996b, MPE Report, 263, 41
Guillout, P., Sterzik, M.F., Schmitt, J.H.M.M., Motch, C., Egret, D., et al., 1998a, A&A 334, 540
Guillout, P., Sterzik, M.F., Schmitt, J.H.M.M., Motch, C., Neuhäuser, R., 1998b, A&A 337, 113
Guillout, P., Sterzik, M.F., 1999, in preparation
Guillout, P., et al., 1999, in preparation
Henry, T.J., Soderblom, D.R., Donahue, R.A., Balinuas, S.L., 1996, AJ 111, 439
Høg, E., 1997, ESA SP-402, 25
Høg, E., Bässgen, G., Bastian, U., Egret, D., Fabricius, C., et al., 1997, A&A 323, L57
Hünsch, M., Schröder, K.P., 1996, A&A 309, L51
Jeffries, R.D., 1995, MNRAS 273, 559
Joy, A.H., 1945, ApJ 102, 168
Krautter, J., Wichmann R., Schmitt, J.H.M.M., Alcalá, J.M., Neuhäuser, R., et al., 1997, A&AS 123, 329
Maccacaro, T., Gioia, I.M., Zamorani, G., Feigelson, E.D., Fener, M., et al., 1982, ApJ 253, 504
Micela, G., Sciortino, S., Vaiana, G.S., Schmitt, J.H.M.M., Stern, R.A., et al., 1988, ApJ 325, 798
Micela, G., Sciortino, S., Vaiana, G.S., Harnden, F.R., Rosner, R., et al., 1990, ApJ 348, 557
Micela, G., Sciortino, S., Favata, F., 1993, ApJ 412, 618
Micela, G., Favata, F., Sciortino, S., 1997, A&A 326, 221
Motch, C., Guillout, P., Haberl, F., Pakull, M., Pietsch, W., et al., 1997, A&A 318, 111
Neuhäuser, R., Torres, G., Sterzik, M.F., Randich, S., 1997, A&A 325, 647
Perryman, M.A.C., Lindegren, L., Kovalevsky, J., Turon, J., Høg, E., et al., 1995, A&A 304, 69
Perryman, M.A.C., Lindegren, L., Kovalevsky, J., Høg, E., Bastian, U., et al., 1997, A&A 323, L49
Pfeffermann, E., Briel V.G., Hippmann H., et al., 1986, SPIE, 733, 519
Pöppel W., 1997, Fundamental of Cosmic Physics, Vol. 18
Rucinski, S.M., Krautter, J., 1983, A&A 121, 217
Schmidt, M., 1968, ApJ 151, 393
Schmitt, J.H.M.M., Golub, L., Harnden, J.F.R., Maxson, C.W., Rosner, R., et al., 1985, ApJ 290, 307
Schmitt, J.H.M.M., 1990, Adv. Space Res., 10, 115
Schmitt, J.H.M.M., 1992, ASP Conf., 26, 83
Schröder, K.P., Hünsch, M., Schmitt, J.H.M.M., 1998, A&A 335, 591
Sciortino, S., Favata, F., Micela, G., 1995, A&A 296, 370
Siess, L., Forestini, M., Dougados, C., 1997, A&A 324, 556
Simon, T., Drake, S.A., 1993, AJ 106, 1660
Simon, T., Drake, S.A., Kim, P.D., 1995, Astr. Soc. Pac., 107, 1034
Soderblom, D.R., King, J.R., Henry, T.J., 1998, AJ 116, 396
Sterzik, M.F., Alcalá, J.M., Neuhäuser, R., Schmitt, J.H.M.M., 1995, A&A 297, 418
Sterzik, M.F., Durisen, R., 1995, A&A 304, L9
Sterzik, M.F., Schmitt, J.H.M.M., 1997, AJ 114, 1673
Stocke, J.T., Morris, S.L., Gioia, I.M., Maccacaro, T., Schild,R., et al., 1991, ApJS 76, 813
Trümper, J., 1983, *Adv. Space. Res.*, 2, 241
Vaiana, G.S., Fabbiano, G., Giacconi, R., Golub, L., Gorenstein, P., et al., 1981, ApJ 245, 163
Voges, W., 1992, in Proceedings of Satellite Symposium 3, “International Space Year Conference”, ESA ISY-3, p9
Voges, W., Aschenbach, B., Boller, Th., et al., 1999, A&A submitted
Wichmann R., Krautter, J., Schmitt, J.H.M.M., Neuhäuser, R., Alcalá, J.M., et al., 1996, A&A 312, 439,
Wichmann R., Sterzik M., Krautter J., Metanomski A., Voges W., 1997, A&A 326, 211
Zickgraf, F.-J., Thiering, I., Krautter, J., et al., 1997, A&AS 123, 103